Technical Note

Institution of MECHANICAL ENGINEERS

Journal of AEROSPACE ENGINEERING

Proc IMechE Part G:
J Aerospace Engineering
0(0) 1–12

DOI: 10.1177/0954410018809468
journals.sagepub.com/home/pig
SAGE

Hybrid frequency domain control for large flexible structures

Xiaoyu Lang[1,2], Christopher J Damaren[2] and Xibin Cao[1]

Abstract

A hybrid finite frequency controller is proposed for the vibration suppression of a large flexible structure mounted with collocated sensors and actuators. The controller has passive characteristics at low frequencies and small gain characteristics at high frequencies. Compared with a strictly positive real controller based on the standard Kalman–Yakubovich–Popov lemma, the hybrid finite frequency controller has less energy consumption but can obtain approximately identical performance. Furthermore, when the plant passivity is violated at high frequencies by noncollocation of sensors and actuators, the strictly positive real controller based on the Kalman–Yakubovich–Popov lemma is no longer able to attenuate the vibration of the large flexible structures, while the hybrid finite frequency controller is effective in suppressing the vibration and avoiding spillover instability. Simulation results are presented to validate the effectiveness of the hybrid finite frequency controller.

Keywords

Flexible structure, vibration control, finite frequency, generalized Kalman–Yakubovich–Popov, passivity

Date received: 5 May 2018; accepted: 4 October 2018

Introduction

Vibration attenuation for large flexible structures has been an attractive academic topic in the past few decades. This problem has many applications such as robotic manipulators,[1–4] flexible spacecraft,[5–8] etc. Specifically, large flexible structures can possess passivity when sensors and actuators are collocated, which is an ideal physical configuration. Input–output stability of passive structures can be provided using the passivity theorem, which states that a closed-loop system is stable if it consists of the negative feedback interconnection of a strictly passive controller and a passive plant. The passivity theorem can be used to show that control of large flexible structures is robust with respect to stiffness and mass modeling errors. However, in practical applications, it is essentially impossible to mount sensors and actuators at exactly the same sites, which is called the noncollocation configuration, and consequently the passivity of the structures is violated. In particular, if the noncollocated sensors and actuators are closely placed, the plant may still be passive in a low-frequency range but may not be passive beyond a certain frequency. For a spacecraft with noncollocation configuration, an experiment-based active damping control approach was addressed to attenuate its flexible appendages.[9] Similar active damping control schemes have been developed for noncollocated dynamic systems.[10–12] A virtual (recalculated) collocation method has been proposed for a flexible rotor to reduce the effects due to noncollocation.[13] A delayed feedback was added into the recurrent wavelet neural network controller to reject disturbance for flexible structures with noncollocated sensors and actuators.[14] However, none of the control schemes in the above literature were developed in the frequency domain for a noncollocated configuration.

To produce a scheme for accommodating passivity violations, the hybrid passive/finite gain stability theorem has been proposed by Forbes.[15] This theorem stemmed from the mixed passive/finite gain stability as addressed in by Griggs.[16,17] It focused on a hybrid system, which maintains passivity in a low-frequency range and has finite gain at high frequencies. At low frequencies, the passive property can permit relatively large gains. At high frequencies, the small gain property can compensate for the inapplicability of the passivity theorem as the passivity is destroyed.

[1]Research Center of Satellite Technology, Harbin Institute of Technology, P. R. China
[2]Institute for Aerospace Studies, University of Toronto, Canada

Corresponding author:
Xiaoyu Lang, Research Center of Satellite Technology, Harbin Institute of Technology, P. O. Box 3012, Harbin 150080, P. R. China.
Email: xylang@hit.edu.cn

As applications of the hybrid passive/finite gain theorem, the hybrid strictly passive/finite gain controllers have been developed to overcome passivity violation caused by the sensor dynamics in robotic manipulator systems.[18,19] These applications were all concentrating on the dynamic systems modeled using all of the finite physical coordinates. In practice, however, common large flexible structures like plates are usually modeled by reduced order models. The modal truncation inevitably separates the real system into a modeled part and an unmodeled part. The unmodeled part makes the hybrid passive/finite gain control of a such a passivity-violated system at high frequencies a serious challenge.

In the field of feedback control, the Kalman–Yakubovich–Popov (KYP) lemma is of crucial importance for stabilization of a nominally passive dynamic system, which has been investigated.[20] However, the KYP lemma primarily deals with the systems which are passive over an infinite frequency range, i.e. have positive real transfer functions. For large flexible structures, the modeled parts usually contain low-frequency modes. It is intuitive that the controllers designed to be passive at low frequencies might be more powerful than the controllers based on the KYP lemma over an infinite frequency range.

The generalized Kalman–Yakubovich–Popov (GKYP) lemma provided a set of linear matrix inequalities (LMIs), which yield a controller designed using distinctive finite frequency ranges.[21,22] Furthermore, the standard KYP lemma fails to accommodate passivity violations since the passivity theorem is not applicable. A fusion of the GKYP lemma and the hybrid passive/finite gain theorem has been implemented to stabilize a single-link manipulator.[19] This motivated us to design a finite-frequency controller using the GKYP lemma to stabilize a partially modeled passivity-violated large flexible structures with robustness to modeling errors, noncollocation, and spillover from the unmodeled parts of the structure (i.e. higher modes).

The contributions of this paper are two-fold. First, we present a finite-frequency controller using the GKYP lemma for a nominally passive large flexible structure and make a comparison with a controller designed by the KYP lemma. Second, it aims to implement the hybrid finite frequency strictly passive/finite gain controller to accommodate passivity violations, which are caused by noncollocation. Numerical simulations are presented at the end to validate the effectiveness of the proposed controller.

Finite frequency control for hybrid passive/finite-gain system

In this section, we will review the concept of passivity in the time and frequency domains individually. The standard KYP lemma and GKYP lemma are presented as well. Then the GKYP lemma is associated with the hybrid passive/finite-gain theorem to construct the controller.

Preliminary

Consider a linear time-invariant (LTI) system

$$\dot{\boldsymbol{x}} = \boldsymbol{A}\boldsymbol{x} + \boldsymbol{B}\boldsymbol{u}, \quad \boldsymbol{y} = \boldsymbol{C}\boldsymbol{x} \tag{1}$$

where $\boldsymbol{x} \in \Re^n$ is the state, $\boldsymbol{y} \in \Re^m$ is the output, $\boldsymbol{u} \in \Re^m$ is the control input. In the time domain, the passivity of the system corresponds to

$$\int_0^T \boldsymbol{y}^T(t)\boldsymbol{u}(t)\mathrm{d}t \geqslant 0, \quad \forall T \geqslant 0, \quad \forall \boldsymbol{u} \in \mathcal{L}_{2e} \tag{2}$$

The system is strictly passive if

$$\begin{gathered}\int_0^T \boldsymbol{y}^T(t)\boldsymbol{u}(t)\,\mathrm{d}t \geqslant \delta \int_0^T \boldsymbol{u}^T\boldsymbol{u}\,\mathrm{d}t \\ (\forall T \geqslant 0, \quad \forall \boldsymbol{u} \in \mathcal{L}_{2e}, \delta > 0)\end{gathered} \tag{3}$$

Taking the Laplace transform in equation (1), the system can be written as $\boldsymbol{y}(s) = \boldsymbol{G}(s)\boldsymbol{u}(s)$, where $\boldsymbol{G}(s) = \boldsymbol{C}(s\mathbf{1} - \boldsymbol{A})^{-1}\boldsymbol{B}$ is the transfer function and $\boldsymbol{y}(s)$ and $\boldsymbol{u}(s)$ are the Laplace transform of $\boldsymbol{y}(t)$ and $\boldsymbol{u}(t)$ respectively. In the frequency domain, the matrix $\boldsymbol{G}(s)$ is positive real if

$$\boldsymbol{G}(j\omega) + \boldsymbol{G}^H(j\omega) \geqslant 0, \quad \forall \omega \in \Re \tag{4}$$

where $(\cdot)^H$ is the complex-conjugate transpose. This is the applicable definition when $\boldsymbol{G}(s)$ has no poles on the imaginary axis. It is well known that the system (1) is passive if $\boldsymbol{G}(s)$ is positive real. An important lemma related to passivity is given as:

Lemma 1. *(KYP lemma) Consider the system* $\boldsymbol{G}(s) = \boldsymbol{C}(s\mathbf{1} - \boldsymbol{A})^{-1}\boldsymbol{B}$ *and assumed that* $\boldsymbol{A}$ *is Hurwitz and* $(\boldsymbol{A}, \boldsymbol{B}, \boldsymbol{C})$ *is a minimal state-space realization. This system is strictly positive real (SPR) if and only if there are matrices* $\boldsymbol{P} = \boldsymbol{P}^T > 0$ *and* $\boldsymbol{Q} = \boldsymbol{Q}^T > 0$ *such that the following conditions are satisfied*:

$$\boldsymbol{P}\boldsymbol{A} + \boldsymbol{A}^T\boldsymbol{P} = -\boldsymbol{Q}, \quad \boldsymbol{P}\boldsymbol{B} = \boldsymbol{C}^T \tag{5}$$

For a proof, see Marquez.[23] The SPR system $\boldsymbol{G}(s)$ corresponds to a strictly passive system if $\boldsymbol{G}(s) = \boldsymbol{C}(s\mathbf{1} - \boldsymbol{A})^{-1}\boldsymbol{B} + \epsilon\mathbf{1}$ for an arbitrarily small $\epsilon > 0$.

The KYP lemma can be used to design an SPR controller. However, the passivity of this controller can be characterized only over an infinite frequency range. In some practical applications, requirements given in the finite frequency ranges are not compatible with the standard KYP lemma. As the extension of this, the GKYP lemma was proposed by Iwasaki.[21,22]

Lemma 2. *(GKYP lemma) Consider the system* $\boldsymbol{G}(s) = \boldsymbol{C}(s\mathbf{1} - \boldsymbol{A})^{-1}\boldsymbol{B}$ *and a given matrix* $\Pi = \Pi^H$.

The following statements are equivalent:[21,22]

(i) Frequency domain condition

$$\begin{bmatrix} \boldsymbol{G}(j\omega) \\ \mathbf{1} \end{bmatrix}^H \Pi \begin{bmatrix} \boldsymbol{G}(j\omega) \\ \mathbf{1} \end{bmatrix} < 0 \tag{6}$$

(ii) Linear matrix inequality: There are two matrices $\boldsymbol{P} = \boldsymbol{P}^T$ *and* $\boldsymbol{Q} = \boldsymbol{Q}^T \geqslant 0$ *such that*

$$\begin{aligned} &\begin{bmatrix} \boldsymbol{A} & \boldsymbol{B} \\ \mathbf{1} & \mathbf{0} \end{bmatrix}^H \boldsymbol{L}(\boldsymbol{P}, \boldsymbol{Q}) \begin{bmatrix} \boldsymbol{A} & \boldsymbol{B} \\ \mathbf{1} & \mathbf{0} \end{bmatrix} \\ &\quad + \begin{bmatrix} \boldsymbol{C} & \mathbf{0} \\ \mathbf{0} & \mathbf{1} \end{bmatrix}^H \Pi \begin{bmatrix} \boldsymbol{C} & \mathbf{0} \\ \mathbf{0} & \mathbf{1} \end{bmatrix} < 0 \end{aligned} \tag{7}$$

Here, the function $\mathbf{L}(\boldsymbol{P}, \boldsymbol{Q})$ *depends on the matrices* $\boldsymbol{P}$ *and* $\boldsymbol{Q}$ *and has particular forms in different frequency ranges which are described below.*

Hybrid passive/finite gain system

For simplicity, the notation $y(j\omega)$ indicates the Fourier transform of a function y. Using Parseval's theorem,[24] a function $y(t) \in \mathcal{L}_2$ if $\int_0^\infty y^2(t)\mathrm{d}t = 1/(2\pi)\,\mathrm{Re}\int_{-\infty}^{\infty} y^H(j\omega)\,y(j\omega)\mathrm{d}\omega < \infty$. The function $y(t) \in \mathcal{L}_{2e}$ if $\int_0^T y^2(t)\mathrm{d}t = 1/(2\pi)\mathrm{Re}\int_{-\infty}^{\infty} y_T^H(j\omega)y_T(j\omega)\mathrm{d}\omega < \infty, 0 \leqslant T < 0$, where $y_T(t) = y(t), 0 \leqslant t \leqslant T$ and $y_T(t) = 0$ when $t > T$. A general negative feedback system is illustrated in Figure 1.

Consider a system $\boldsymbol{y} = \mathcal{G}\boldsymbol{e}$ where the operator $\mathcal{G}$: $\mathcal{L}_{2e} \rightarrow \mathcal{L}_{2e}$. The definitions of a hybrid passive/finite gain system are given as follows:[15]

Definition 1. *A hybrid passive/finite gain system* $\mathcal{G}$ *satisfies*

$$\begin{aligned} &\frac{1}{2\pi}\int_{-\infty}^{\infty} \boldsymbol{y}_T^H(j\omega)\boldsymbol{Q}(\omega)\boldsymbol{y}_T(j\omega)\mathrm{d}\omega \\ &\quad + \frac{1}{\pi}\int_{-\infty}^{\infty} \boldsymbol{y}_T^H(j\omega)\boldsymbol{S}(\omega)\boldsymbol{e}_T(j\omega)\mathrm{d}\omega \\ &\quad + \frac{1}{2\pi}\int_{-\infty}^{\infty} \boldsymbol{e}_T^H(j\omega)\boldsymbol{R}(\omega)\boldsymbol{e}_T(j\omega)\mathrm{d}\omega \geqslant 0 \end{aligned} \tag{8}$$

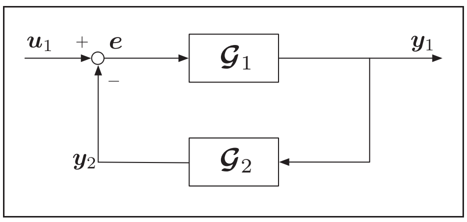

Figure 1. General negative feedback system.

where

$$\begin{aligned} \boldsymbol{Q}(\omega) &= -\left[\epsilon\alpha(\omega) + \gamma^{-1}(1 - \alpha(\omega))\right]\mathbf{1} \\ \boldsymbol{S}(\omega) &= \frac{1}{2}\alpha(\omega)\mathbf{1} \\ \boldsymbol{R}(\omega) &= [\gamma(1 - \alpha(\omega) - \delta\alpha(\omega)]\mathbf{1} \end{aligned} \tag{9}$$

The constant parameters ϵ, δ describe the system's passivity properties. The constant γ describes the finite gain of the system. The purpose of the variable α is to split the entire frequency range into two sub-ranges

$$\alpha(\omega) = \begin{cases} 1, & -\omega_c \leqslant \omega \leqslant \omega_c \quad (\textit{passive region}) \\ 0, & |\omega| > \omega_c \quad (\textit{finite gain region}) \end{cases} \tag{10}$$

where ω_c will be called the critical frequency.

By considering the case $-\omega_c \leqslant \omega \leqslant \omega_c$ with $\alpha(\omega) = 1$ and $|\omega| > \omega_c$ with $\alpha(\omega) = 0$, equation (8) can be satisfied if

$$\begin{aligned} &\frac{1}{2\pi}\mathrm{Re}\int_{-\omega_c}^{\omega_c} \boldsymbol{y}_T^H(j\omega)\boldsymbol{e}_T(j\omega)\mathrm{d}\omega \\ &\quad \geqslant \frac{\epsilon}{2\pi}\int_{-\omega_c}^{\omega_c} \boldsymbol{y}_T^H(j\omega)\boldsymbol{y}_T(j\omega)\mathrm{d}\omega \\ &\quad + \frac{\delta}{2\pi}\int_{-\omega_c}^{\omega_c} \boldsymbol{e}_T^H(j\omega)\boldsymbol{e}_T(j\omega)\mathrm{d}\omega \end{aligned} \tag{11}$$

and

$$\frac{1}{\pi\gamma}\int_{\omega_c}^{\infty} \boldsymbol{y}_T^H(j\omega)\boldsymbol{y}_T(j\omega)\mathrm{d}\omega \leqslant \frac{\gamma}{\pi}\int_{\omega_c}^{\infty} \boldsymbol{e}_T^H(j\omega)\boldsymbol{e}_T(j\omega)\mathrm{d}\omega \tag{12}$$

In equation (11), passive characteristics is possessed at low frequency whereas equation (12) expresses finite gain at high frequency, i.e. $\sigma_{\max}\{\boldsymbol{G}(j\omega)\} \leqslant \gamma$ for $|\omega| > \omega_c$.

We now invoke the GKYP lemma in equation (7). If a LTI system has passive characteristics for $-\omega_c \leqslant \omega \leqslant \omega_c$, it was shown by Iwasaki,[22] that

$$\Pi = \begin{bmatrix} \mathbf{0} & -\mathbf{1} \\ -\mathbf{1} & \mathbf{0} \end{bmatrix}$$

makes equation (6) equivalent to equation (11). Then taking

$$\boldsymbol{L}(\boldsymbol{P}, \boldsymbol{Q}) = \begin{bmatrix} -\boldsymbol{Q} & \boldsymbol{P} \\ \boldsymbol{P} & \omega_c^2\boldsymbol{Q} \end{bmatrix}$$

one can express (7) as

$$\begin{aligned} &\begin{bmatrix} \boldsymbol{A} & \boldsymbol{B} \\ \mathbf{1} & \mathbf{0} \end{bmatrix}^H \begin{bmatrix} -\boldsymbol{Q} & \boldsymbol{P} \\ \boldsymbol{P} & \omega_c^2\boldsymbol{Q} \end{bmatrix} \begin{bmatrix} \boldsymbol{A} & \boldsymbol{B} \\ \mathbf{1} & \mathbf{0} \end{bmatrix} \\ &\quad + \begin{bmatrix} \boldsymbol{C} & \mathbf{0} \\ \mathbf{0} & \mathbf{1} \end{bmatrix}^H \begin{bmatrix} \mathbf{0} & -\mathbf{1} \\ -\mathbf{1} & \mathbf{0} \end{bmatrix} \begin{bmatrix} \boldsymbol{C} & \mathbf{0} \\ \mathbf{0} & \mathbf{1} \end{bmatrix} \leqslant 0 \end{aligned} \tag{13}$$

If the LTI system is SPR over $-\omega_c \leqslant \omega \leqslant \omega_c$, the inequality (7) can be given by

$$\begin{aligned}&\begin{bmatrix} \boldsymbol{A} & \boldsymbol{B} \\ \boldsymbol{1} & \boldsymbol{0} \end{bmatrix}^H \begin{bmatrix} -\boldsymbol{Q} & \boldsymbol{P} \\ \boldsymbol{P} & \omega_c^2 \boldsymbol{Q} \end{bmatrix} \begin{bmatrix} \boldsymbol{A} & \boldsymbol{B} \\ \boldsymbol{1} & \boldsymbol{0} \end{bmatrix} \\ &\quad + \begin{bmatrix} \boldsymbol{C} & \boldsymbol{0} \\ \boldsymbol{0} & \boldsymbol{1} \end{bmatrix}^H \begin{bmatrix} \boldsymbol{0} & -\boldsymbol{1} \\ -\boldsymbol{1} & \boldsymbol{0} \end{bmatrix} \begin{bmatrix} \boldsymbol{C} & \boldsymbol{0} \\ \boldsymbol{0} & \boldsymbol{1} \end{bmatrix} < 0\end{aligned} \tag{14}$$

Equation (6) represents equation (12) if we take

$$\Pi = \begin{bmatrix} \boldsymbol{1} & \boldsymbol{0} \\ \boldsymbol{0} & -\gamma^2 \boldsymbol{1} \end{bmatrix}$$

The corresponding choice for $\boldsymbol{L}(\boldsymbol{P}, \boldsymbol{Q})$ in equation (12) is

$$\boldsymbol{L}(\boldsymbol{P}, \boldsymbol{Q}) = \begin{bmatrix} \boldsymbol{Q} & \boldsymbol{P} \\ \boldsymbol{P} & -\omega_c^2 \boldsymbol{Q} \end{bmatrix}$$

so that equation (7) becomes

$$\begin{aligned}&\begin{bmatrix} \boldsymbol{A} & \boldsymbol{B} \\ \boldsymbol{1} & \boldsymbol{0} \end{bmatrix}^H \begin{bmatrix} \boldsymbol{Q} & \boldsymbol{P} \\ \boldsymbol{P} & -\omega_c^2 \boldsymbol{Q} \end{bmatrix} \begin{bmatrix} \boldsymbol{A} & \boldsymbol{B} \\ \boldsymbol{1} & \boldsymbol{0} \end{bmatrix} \\ &\quad + \begin{bmatrix} \boldsymbol{C} & \boldsymbol{0} \\ \boldsymbol{0} & \boldsymbol{1} \end{bmatrix}^H \begin{bmatrix} \boldsymbol{1} & \boldsymbol{0} \\ \boldsymbol{0} & -\gamma^2 \boldsymbol{1} \end{bmatrix} \begin{bmatrix} \boldsymbol{C} & \boldsymbol{0} \\ \boldsymbol{0} & \boldsymbol{1} \end{bmatrix} < 0\end{aligned} \tag{15}$$

Stability

In the above section, the critical frequency ω_c plays a dominant role in a hybrid system definition. It is the division between the passive and finite gain region. The critical frequency ω_c of the plant system is assumed to be known in the following. The GKYP lemma can be implemented for a hybrid system with its corresponding properties in different frequency ranges. The stability can be ensured by the hybrid passivity/finite gain theorem presented in Forbes.[15]

Theorem 1. (Hybrid passivity finite gain theorem) *Consider the two systems* $\mathcal{G}_1 : \mathcal{L}_{2e} \to \mathcal{L}_{2e}$ *and* $\mathcal{G}_2 : \mathcal{L}_{2e} \to \mathcal{L}_{2e}$ *interconnected with negative feedback as illustrated in Figure 1. Assumed these two systems are hybrid passivity/finite gain system with corresponding parameters as* $\mathcal{G}_1 : \delta_1, \epsilon_1, \gamma_1$ *and* $\mathcal{G}_2 : \delta_2, \epsilon_2, \gamma_2$ *satisfying (11) and (12). The interconnected system with* $\mathcal{G}_1$ *and* $\mathcal{G}_2$ *is* $\mathcal{L}_2$ *stable if* $\delta_1 + \epsilon_2 > 0$, $\delta_2 + \epsilon_1 > 0$ *and* $\gamma_1\gamma_2 < 1$.

For a proof, see Forbes.[15]

Application to large flexible structures

The main application in this paper is a large rectangular plate. The dynamic structure is shown in Figure 2. The plate is assumed to be a thin plate satisfying the Kirchhoff plate theory. The finite element method (FEM) is used as the numerical approach to build the dynamic equations. The rectangular element is employed in the FEM. The rectangular plate is cantilevered at the center point, which removes the rigid body modes. Each node has three degrees of freedom (w, w_x, w_y), where w is the vertical displacement of the node and $w_x = \partial w/\partial x, w_y = \partial w/\partial y$ indicate two rotations of the node with respect to $(-y)$-axis and x-axis respectively. For each four-node element, the degrees of freedom $\boldsymbol{q}_{ee}$ can be given as

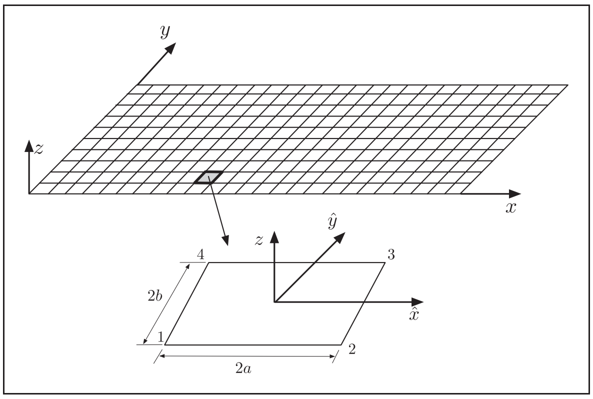

Figure 2. Dynamic model.

$$\boldsymbol{q}_{ee} = [w_1, w_{x1}, w_{y1}, \ldots, w_4, w_{x4}, w_{y4}]^T \tag{16}$$

The twelve-term polynomial describing $w(x, y, t)$ in each element is given by

$$w(\hat{x}, \hat{y}, t) = \boldsymbol{N}(\hat{x}, \hat{y})\boldsymbol{q}_{ee}(t) \tag{17}$$

where $\boldsymbol{N}(\hat{x}, \hat{y})$ is suitably chosen and $\hat{x}$ and $\hat{y}$ are given by

$$\hat{x} = \frac{x}{a}, \quad \hat{y} = \frac{y}{b} \tag{18}$$

For the rectangular plate with mass density per unit volume ρ and thickness h, the kinetic energy of an element is given as

$$\begin{aligned} T_e &= \frac{1}{2} \int\int_{A_e} \rho h \dot{w}^2 \mathrm{d}A \\ &= \frac{1}{2}\rho h \int\int_{A_e} \dot{\boldsymbol{q}}_{ee}^T \boldsymbol{N}^T \boldsymbol{N} \dot{\boldsymbol{q}}_{ee} \mathrm{d}A \\ &= \frac{1}{2} \dot{\boldsymbol{q}}_{ee}^T \boldsymbol{m}_{ee} \dot{\boldsymbol{q}}_{ee} \end{aligned} \tag{19}$$

where

$$\boldsymbol{m}_{ee} = \rho h \int\int_{A_e} \boldsymbol{N}^T \boldsymbol{N} \mathrm{d}A \tag{20}$$

The potential energy is given by

$$U_e = \frac{1}{2} D \int\int_{A_e} \left[w_{xx}^2 + w_{yy}^2 + 2w_{xx}w_{yy} + 2(1-\gamma_p)w_{xy}^2 \right] \mathrm{d}A$$
$$= \frac{1}{2} \boldsymbol{q}_{ee}^T \boldsymbol{k}_{ee} \boldsymbol{q}_{ee} \tag{21}$$

where

$$\boldsymbol{k}_{ee} = D \int\int_{A_e} \left[\boldsymbol{N}_{xx}^T \boldsymbol{N}_{xx} + \boldsymbol{N}_{yy}^T \boldsymbol{N}_{yy} + \boldsymbol{N}_{xx}^T \boldsymbol{N}_{yy} + \boldsymbol{N}_{yy}^T \boldsymbol{N}_{xx} + 2(1-\gamma_p) \boldsymbol{N}_{xy}^T \boldsymbol{N}_{xy} \right] \mathrm{d}A \tag{22}$$

The rigidity D is defined as $D = Eh^3/(12(1-\gamma_p^2))$, where E is the Young's modulus, and γ_p is the Poisson's ratio.

The global mass matrix $\boldsymbol{M}_g$ and stiffness matrix $\boldsymbol{K}_g$ can be assembled using the standard FEM procedures. Therefore, the dynamic equation of the rectangular plate can be yielded as

$$\boldsymbol{M}_g \ddot{\boldsymbol{q}} + \boldsymbol{K}_g \boldsymbol{q} = \boldsymbol{b} \boldsymbol{u} \tag{23}$$

where $\boldsymbol{q}$ is the global vector, which contains the vertical displacement w and two-axis rotations (w_x, w_y) for all of the nodes. The input matrix $\boldsymbol{b}$ indicates the positions of the actuators used on the plate. The output equation is

$$\boldsymbol{y} = \boldsymbol{c} \dot{\boldsymbol{q}} \tag{24}$$

where the output matrix $\boldsymbol{c}$ indicates positions of the rate sensors on the plate.

The eigenproblem of the unforced equation in equation (23) is

$$\left(-\omega_\alpha^2 \boldsymbol{M}_g + \boldsymbol{K}_g\right) \boldsymbol{q}_\alpha = 0, \quad \alpha = 1, 2, 3, \ldots \tag{25}$$

where ω_α are the natural frequencies. The eigenvectors $\boldsymbol{q}_\alpha$ can be normalized according to

$$\boldsymbol{q}_\alpha^T \boldsymbol{M}_g \boldsymbol{q}_\beta = \delta_{\alpha\beta}, \quad \boldsymbol{q}_\alpha^T \boldsymbol{K}_g \boldsymbol{q}_\beta = \omega_\alpha^2 \delta_{\alpha\beta}$$

where $\delta_{\alpha\beta}$ is the Kronecker delta. We expand the global vector as $\boldsymbol{q}(t) = \sum_{\alpha=1}^{n} \boldsymbol{q}_\alpha \eta_\alpha(t)$ to get decoupled equations like

$$\begin{aligned} &\ddot{\eta}_\alpha + 2\zeta_\alpha \omega_\alpha \dot{\eta}_\alpha + \omega_\alpha^2 \eta_\alpha = \widehat{\boldsymbol{B}}_\alpha \boldsymbol{u} \\ &\widehat{\boldsymbol{B}}_\alpha = \boldsymbol{q}_\alpha^T \boldsymbol{b}, \quad \alpha = 1, 2, 3, \ldots, n \end{aligned} \tag{26}$$

where n is the number of degrees of freedom in the FEM, and ζ_α are the modal damping factors introduced at this step to indicate viscous damping. It is reasonable to add damping since damping effects exist in almost all materials. The modal coordinates are used to form the state

$$\boldsymbol{x} = \mathrm{col}\{\boldsymbol{\eta}, \dot{\boldsymbol{\eta}}\}, \boldsymbol{\eta} = [\eta_1 \quad \eta_2 \quad \cdots \quad \eta_n]^T$$

The output in equation (24) can be written as

$$\boldsymbol{y} = \sum_{\alpha=1}^{n} \widehat{\boldsymbol{C}}_\alpha \dot{\eta}_\alpha, \quad \widehat{\boldsymbol{C}}_\alpha = \boldsymbol{c}\boldsymbol{q}_\alpha \tag{27}$$

The state-space model can be established as in equation (1) where

$$\begin{aligned} &\boldsymbol{A} = \begin{bmatrix} \boldsymbol{0} & \boldsymbol{1} \\ -\Omega^2 & -\widehat{\boldsymbol{D}} \end{bmatrix}, \Omega = \mathrm{diag}\{\omega_\alpha\} \\ &\widehat{\boldsymbol{D}} = \mathrm{diag}\{2\zeta_\alpha\omega_\alpha\}, \quad \boldsymbol{B} = \begin{bmatrix} \boldsymbol{0} \\ \widehat{\boldsymbol{B}} \end{bmatrix}, \quad \widehat{\boldsymbol{B}} = \mathrm{col}\left\{\widehat{\boldsymbol{B}}_\alpha\right\}, \\ &\boldsymbol{C} = \left[\boldsymbol{0}\ \widehat{\boldsymbol{C}}\right], \quad \widehat{\boldsymbol{C}} = \mathrm{row}\left\{\widehat{\boldsymbol{C}}_\alpha\right\} \end{aligned} \tag{28}$$

Main results for controller design

This section considers the design of a controller for the rectangular plate. In the above section, the exact positions of the actuators and sensors were not prescribed. There are two options: one is collocation, in which the rate sensors and force actuators are mounted at the same places. This is ideal for large flexible structures control, since the plant maintains passivity. The other one is noncollocation, which means these two are laid at different places. In this case, the passivity violation happens at this condition. The controllers designed in this paper will target these two situations individually.

Case A: Plate with collocated sensors and actuators

The scheme of a rectangular plate used in this case is also shown in Figure 3. The sensor and actuator are collocated on the first corner of the rectangular plate. As a result, the rectangular plate is a passive system where $\boldsymbol{c} = \boldsymbol{b}^T$. One form of the passivity theorem states that a passive system can be stabilized if it is interconnected in negative feedback with an SPR controller. Following this theorem, the basic idea for controller design is to arrive at an SPR controller. In this

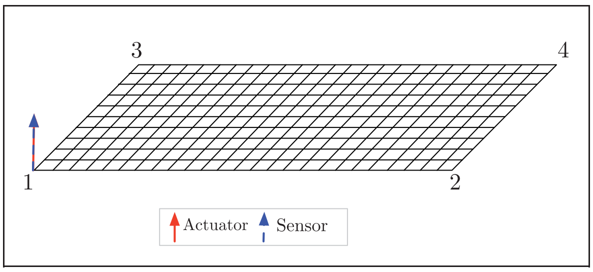

Figure 3. Plate with collocated sensors and actuators.

case, the controller is set as

$$\boldsymbol{x}_c = \boldsymbol{A}_c\boldsymbol{x}_c + \boldsymbol{B}_c\boldsymbol{u}_c, \quad \boldsymbol{y}_c = \boldsymbol{C}_c\boldsymbol{x}_c \tag{29}$$

where $\boldsymbol{x}_c$ is the state of this controller, $\boldsymbol{y}_c$ is the output of the controller. Since negative feedback is used, $\boldsymbol{y}_c = -\boldsymbol{u}$ and $\boldsymbol{y} = \boldsymbol{u}_c$. The standard KYP lemma shown as Lemma 1 is a good approach to obtain a controller which maintains strictly positive realness. Motivated by Benhabib,[20] the value of the gain $\boldsymbol{C}_c$ is obtained as the state feedback gain from the linear quadratic regulator (LQR) with suitable selection of the weight matrices $\boldsymbol{Q} = \boldsymbol{Q}^T > 0$ and $\boldsymbol{R} = \boldsymbol{R}^T > 0$ along with matrices $\boldsymbol{A}$ and $\boldsymbol{B}$ in the system in equation (1) as well. A Hurwitz matrix $\boldsymbol{A}_c$ can be set as

$$\boldsymbol{A}_c = \boldsymbol{A} - \boldsymbol{B}\boldsymbol{C}_c \tag{30}$$

Substituting $\boldsymbol{A}_c$ into equation (5) with suitable $\boldsymbol{Q}_c = \boldsymbol{Q}_c^T > 0$, we can find $\boldsymbol{P}_c$ by solving

$$\boldsymbol{P}_c\boldsymbol{A}_c + \boldsymbol{A}_c^T\boldsymbol{P}_c = -\boldsymbol{Q}_c \tag{31}$$

Then

$$\boldsymbol{B}_c = \boldsymbol{P}_c^{-1}\boldsymbol{C}_c^T \tag{32}$$

An SPR controller $\boldsymbol{G}_1(s) = \boldsymbol{C}_c(s\mathbf{1} - \boldsymbol{A}_c)^{-1}\boldsymbol{B}_c$ results on the basis of the standard KYP lemma. However, this design process is accomplished in the time domain which implies that passivity is achieved over the entire frequency range. The gain at high-frequency range is not taken into account. It might lead to a relative large gain for the controller, which is undesirable in real practical applications. For the rectangular plate used in this paper, the state-space equation used for controller design results from modal truncation at a certain order. In fact, the states of the plant in equation (1) only contain the low-frequency entries of the modal coordinates $\boldsymbol{\eta}$. This provides a possibility for designing a controller for the low-frequency range rather than the entire frequency range.

The basic idea is dividing the entire frequency range into two parts using the critical frequency ω_c, namely low- and high-frequency ranges. The form of the controller in equation (29) designed in this case will be maintained in these two frequency ranges. The computational process for the matrices $\boldsymbol{A}_c$ and $\boldsymbol{B}_c$ is identical with equations (30) to (32). The output gain of the controller is renamed as $\boldsymbol{K}$. The new controller designed using finite frequency ranges is denoted by $\boldsymbol{G}_2(s) = \boldsymbol{K}(s\mathbf{1} - \boldsymbol{A}_c)^{-1}\boldsymbol{B}_c$.

We design the controller to be SPR at low frequencies. Recall equation (7) in the GKYP lemma mentioned in Lemma 2, the controller is SPR when $\omega \leqslant \omega_c$ if

$$\begin{bmatrix} \boldsymbol{A}_c & \boldsymbol{B}_c \\ \mathbf{1} & \mathbf{0} \end{bmatrix}^H \begin{bmatrix} -\boldsymbol{Q}_l & \boldsymbol{P}_l \\ \boldsymbol{P}_l & \omega_c^2\boldsymbol{Q}_l \end{bmatrix} \begin{bmatrix} \boldsymbol{A}_c & \boldsymbol{B}_c \\ \mathbf{1} & \mathbf{0} \end{bmatrix} + \begin{bmatrix} \boldsymbol{K} & \mathbf{0} \\ \mathbf{0} & \mathbf{1} \end{bmatrix}^H \begin{bmatrix} \mathbf{0} & -\mathbf{1} \\ -\mathbf{1} & \mathbf{0} \end{bmatrix} \begin{bmatrix} \boldsymbol{K} & \mathbf{0} \\ \mathbf{0} & \mathbf{1} \end{bmatrix} < 0 \tag{33}$$

where $\boldsymbol{P}_l = \boldsymbol{P}_l^T$ and $\boldsymbol{Q}_l = \boldsymbol{Q}_l^T > 0$. The variables in the LMI are $\boldsymbol{K}$, $\boldsymbol{P}_l$, and $\boldsymbol{Q}_l$. Even though the plant state-space equation using modal coordinates concentrates on the low-frequency modes, the real plate system contains the entire frequency range. The constraint on $\boldsymbol{K}$ in the LMI in equation (33) is not sufficient for designing the high-frequency range. An extra constraint is proposed for the high-frequency range.

In the high-frequency range $|\omega| > \omega_c$, the gain γ_2 should be finite, which implies the controller system is bounded real. By using Theorem 1, the gain $\gamma_2 < 1/\gamma_1$ where, recall γ_1 is the high frequency gain of the plant. Recalling equation (15) in Lemma 2, the controller is bounded real when $|\omega| > \omega_c$ if

$$\begin{bmatrix} \boldsymbol{A}_c & \boldsymbol{B}_c \\ \mathbf{1} & \mathbf{0} \end{bmatrix}^H \begin{bmatrix} \boldsymbol{Q}_h & \boldsymbol{P}_h \\ \boldsymbol{P}_h & -\omega_c^2\boldsymbol{Q}_h \end{bmatrix} \begin{bmatrix} \boldsymbol{A}_c & \boldsymbol{B}_c \\ \mathbf{1} & \mathbf{0} \end{bmatrix} + \begin{bmatrix} \boldsymbol{K} & \mathbf{0} \\ \mathbf{0} & \mathbf{1} \end{bmatrix}^H \begin{bmatrix} \mathbf{1} & \mathbf{0} \\ \mathbf{0} & -\gamma_2^2\mathbf{1} \end{bmatrix} \begin{bmatrix} \boldsymbol{K} & \mathbf{0} \\ \mathbf{0} & \mathbf{1} \end{bmatrix} < 0 \tag{34}$$

Noticing that the left hand side of equation (34) contains a nonlinear term with respect to $\boldsymbol{K}$, the Schur complement is employed to transform equation (34) into equation (35).

$$\begin{bmatrix} \left\{ \begin{matrix} \boldsymbol{A}_c^T\boldsymbol{Q}_h\boldsymbol{A}_c + \boldsymbol{P}_h\boldsymbol{A}_c \\ +\boldsymbol{A}_c^T\boldsymbol{P}_h - \omega_c^2\boldsymbol{Q}_h \end{matrix} \right\} & \boldsymbol{A}_c^T\boldsymbol{Q}_h\boldsymbol{B}_c + \boldsymbol{P}_h\boldsymbol{B}_c & \boldsymbol{K}^T \\ \text{sym} & \boldsymbol{B}_c^T\boldsymbol{Q}_h - \gamma_2^2\mathbf{1} & \mathbf{0} \\ \text{sym} & \text{sym} & -\mathbf{1} \end{bmatrix} < 0 \tag{35}$$

The variables in the LMI in equation (35) are $\boldsymbol{K}$, $\boldsymbol{P}_h = \boldsymbol{P}_h^T$ and $\boldsymbol{Q}_h = \boldsymbol{Q}_h^T > 0$. This controller is a hybrid passive/finite gain system, which can stabilize the passive rectangular plate system (1) along with Theorem 1 if the gain $\boldsymbol{K}$ satisfies the two constraints shown in the LMIs in equations (33) and (35). However, feasible solutions of LMIs (33) and (35) might not be unique. Optimization is an applicable approach to obtain an exclusive solution for gain $\boldsymbol{K}$. We choose an objective function to be minimized

$$\mathcal{J} = \mathrm{tr}[(\boldsymbol{K} - \boldsymbol{C}_c)(\boldsymbol{K} - \boldsymbol{C}_c)^T] \tag{36}$$

This objective function will force the controller designed with the GKYP lemma to mimic the controller from the standard KYP lemma.

Using similar means in Forbes[19] for solving the LMIs, an additional variable $\boldsymbol{Z} = \boldsymbol{Z}^T \geqslant 0$ is introduced and two additional constraints are employed as

$$\mathrm{tr}[\boldsymbol{Z}] \leqslant \mathcal{J} \tag{37a}$$

$$(\boldsymbol{K}-\boldsymbol{C}_c)(\boldsymbol{K}-\boldsymbol{C}_c)^T \leqslant \boldsymbol{Z} \tag{37b}$$

These additional constraints are logical since minimal $\mathcal{J}$ implies minimal tr[$\boldsymbol{Z}$] as $(\boldsymbol{K}-\boldsymbol{C}_c)(\boldsymbol{K}-\boldsymbol{C}_c)^T$ is being minimized. Since the left hand of equation (37b) is nonlinear in $\boldsymbol{K}$, the Schur complement is used to transform it as

$$-\begin{bmatrix} \boldsymbol{Z} & (\boldsymbol{K}-\boldsymbol{C}_c)^T \\ \text{sym} & \boldsymbol{1} \end{bmatrix} \leqslant 0 \tag{38}$$

The optimal $\boldsymbol{K}$ can be determined from following optimization problem

$$\begin{aligned} &\min && \mathcal{J}(\boldsymbol{K}, \boldsymbol{P}_l, \boldsymbol{Q}_l, \boldsymbol{P}_h, \boldsymbol{Q}_h, \boldsymbol{Z}) \\ &\text{subject to} && \text{LMIs in (33), (35), (38)} \end{aligned} \tag{39}$$

Up to here, a hybrid SPR/finite gain controller $\boldsymbol{G}_2 = \boldsymbol{K}(s\boldsymbol{1}-\boldsymbol{A}_c)^{-1}\boldsymbol{B}_c$ has been determining using the GKYP lemma and the optimization algorithm simultaneously.

Case B: Plate with noncollocated sensors and actuators

In this case, the rectangular plate is equipped with noncollocated sensors and actuators, as shown in Figure 4. The sensor and actuator are placed at different positions. In this case, the sensor's site is assumed to be not too far away from the actuator's location, which implies that passivity is maintained by the plant below a critical frequency ω_c but it would be violated beyond ω_c. The plant has passive characteristics only in a low-frequency range rather than the entire frequency range. Therefore, the controller (29) based on the standard KYP lemma is pointless since it is incompatible with the passivity theorem. In this sense, the advantage is apparent if the hybrid passive/finite gain controller is designed under the GKYP lemma. The passivity violation at high-frequency range can be accommodated by estimating an upper bound on the plant gain beyond ω_c.

Since the controller $\boldsymbol{G}_1$ based on the standard KYP lemma is not suitable in this case, the optimization problem is abandoned. The gain $\boldsymbol{K}$ of the controller $\boldsymbol{G}_2 = \boldsymbol{K}(s\boldsymbol{1}-\boldsymbol{A}_c)^{-1}\boldsymbol{B}_c$ is obtained directly by solving the LMIs (33) and (35) instead of equation (39). Therefore, the solution of the gain $\boldsymbol{K}$ is not unique without the optimization used in Case A. The computation processes of parameters $\boldsymbol{A}_c$ and $\boldsymbol{B}_c$ remains the same as in Case A.

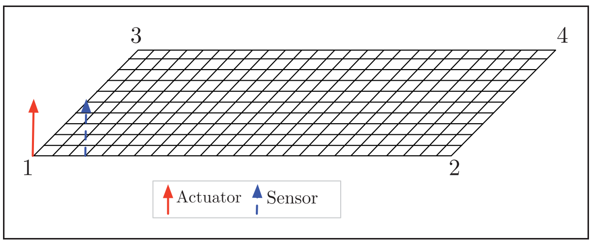

Figure 4. Plate with noncollocated sensors and actuator.

Simulations and discussions

In this section, two numerical simulation results are given to show the improvement provided by the controller based on the GKYP lemma. The common initial parameters for simulation are set first. The rectangular plate is cantilevered at the center point. The displacement w_{center} and rotations $w_x(center), w_y(center)$ of the central node are zeros for all time, which are the boundary conditions. This effectively removes the rigid body modes. The dynamics in equation (23) are built using the FEM with the parameters $E = 2.1 \times 10^{11}\,\text{Pa}$, $\gamma_p = 0.3$, $\rho = 2.7 \times 10^3\,\text{kg/m}^3$, and $h = 0.01\,\text{m}$. The size of the plate is $2.5\text{m} \times 2\text{m}$. The mesh has 21×21 nodes for the plate in the FEM. When a force 5N is applied on the fourth corner labeled as in Figures 2 and 4, the initial coordinates for the vertical displacement of all nodes can be obtained from

$$\boldsymbol{q}_{\text{initial}} = \boldsymbol{K}_g^{-1}\boldsymbol{P} \tag{40}$$

where $\boldsymbol{P}$ is all zeros except for a one corresponding to the force location.

Simulation for Case A

Case A aims at a plate with collocated sensors and actuators. One sensor and one actuator are placed at the first corner, which is shown in Figure 2. Since the actuator is placed at the first node of the plate, $\boldsymbol{b} = [1, \underbrace{0, \ldots, 0}_{n-1}]^T$. The collocation leads to $\boldsymbol{c} = \boldsymbol{b}^T$. For the modal equations (26), the first 13 modal equations are used to build the state-space equation in (1)

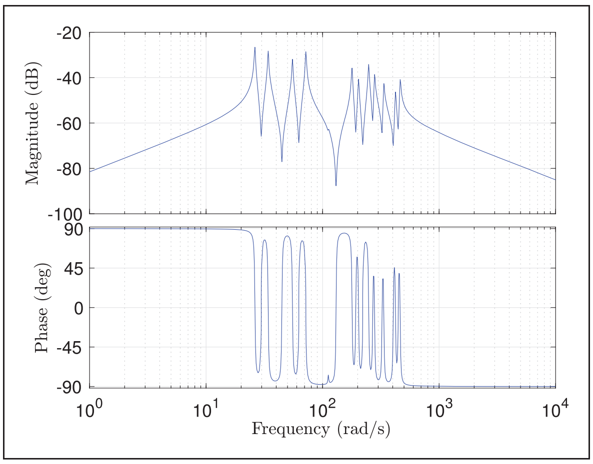

Figure 5. Frequency response of the plant.

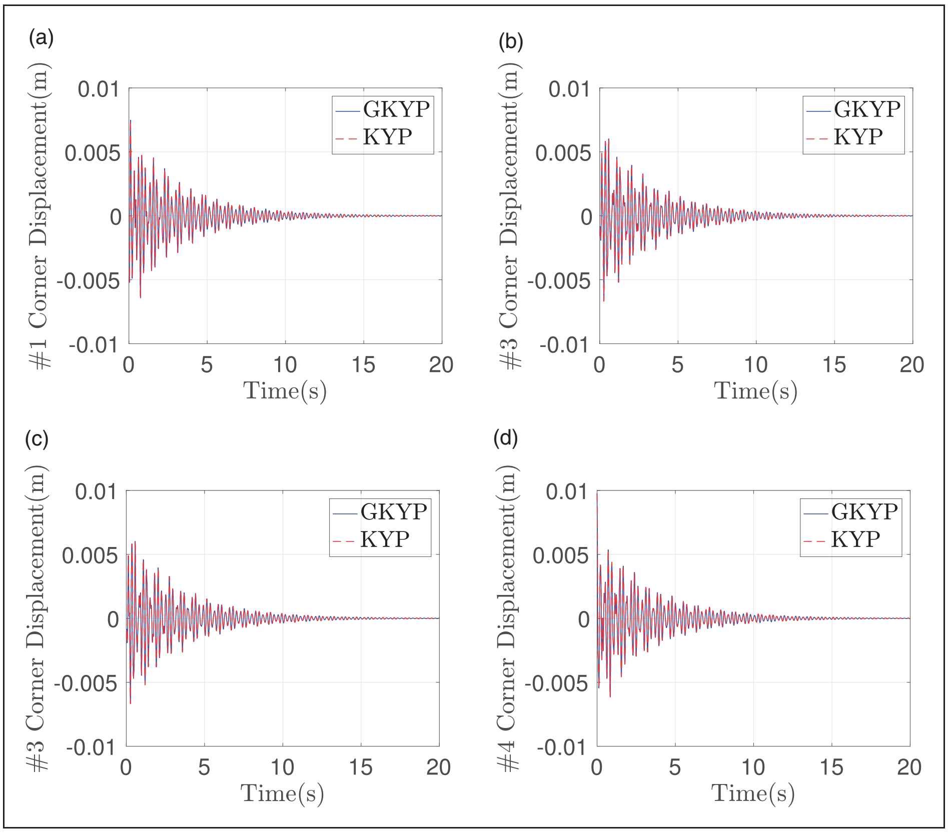

Figure 6. Displacements of four plate corners: (a) #1 corner; (b) #2 corner; (c) #3 corner; (d) #4 corner.

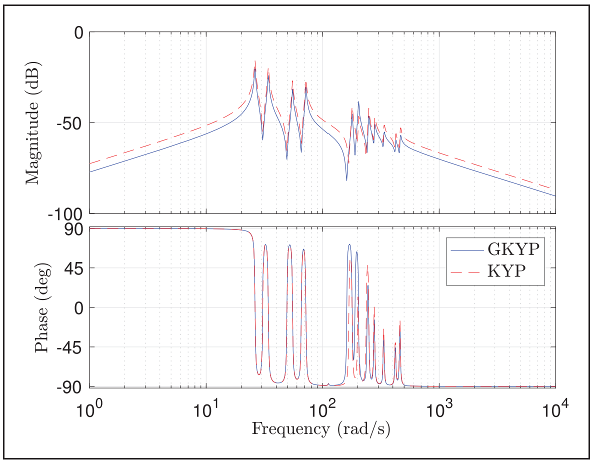

Figure 7. Frequency response of controllers GKYP and KYP.

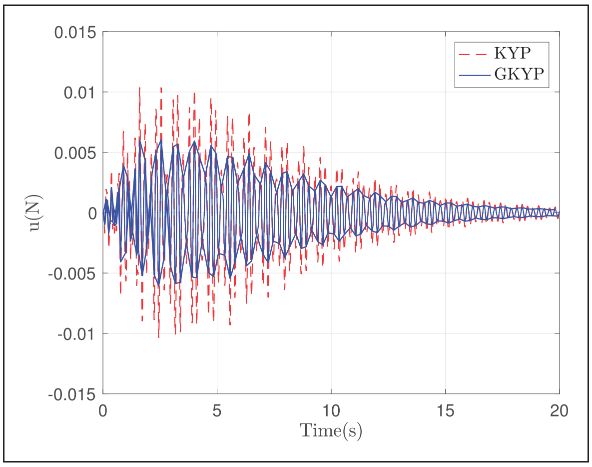

Figure 8. Control force.

with the damping $\zeta = 0.01$. The bode plot of the rectangular plate is shown in Figure 5. It is obvious that the plant is passive since the phase shift is always in $[-90^\circ, 90^\circ]$. Controller A satisfying the standard KYP lemma (KYP controller) and controller B satisfying the GKYP lemma (GKYP controller) are applied to generate a comparison between them. First, we choose the weights of the LQR algorithm with $\boldsymbol{Q} = 1 \times \mathbf{1}$, $\boldsymbol{Q}_c = 1 \times \mathbf{1}$, and $\boldsymbol{R} = 0.5 \times \mathbf{1}$, where $\mathbf{1}$ is an identity matrix with suitable size required by the LQR algorithm. The parameters of the KYP controller are computed by the standard KYP lemma. The GKYP controller is designed with parameters $\omega_c = 202.5358\,\text{rad/s}$ and $\gamma_2 = 2.2492$. The parameters $\boldsymbol{A}_c$ and $\boldsymbol{B}_c$ are same as the KYP controller.

Figure 6 depicts approximately the identical time response of the displacement of the four plate corners for the KYP controller and the GKYP controller. The identical performance validates the effectiveness of the GKYP controller. The frequency responses for these two controllers are shown in Figure 7. The GKYP controller has smaller gain compared with the KYP controller. This advantageous feature is clearly depicted in Figure 8 which shows the control force. The gain of GKYP controller has lower peak values than the gain in KYP controller. It is more straightforward if defining an energy-consumption norm Ec as

$$Ec = \frac{1}{t_f}\sqrt{\int_0^{t_f} \boldsymbol{u}^T \boldsymbol{u} \mathrm{d}t} \tag{41}$$

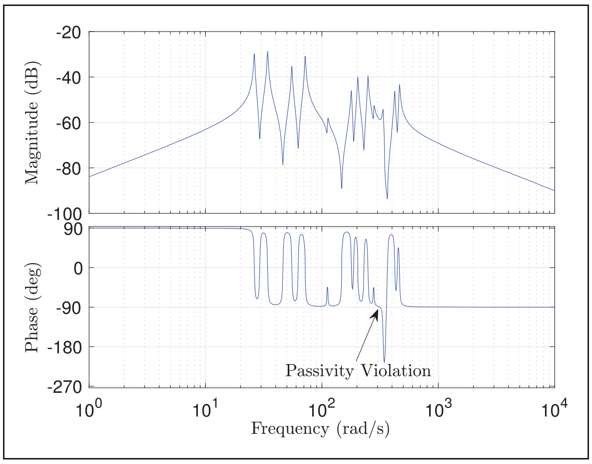

Figure 9. Frequency response of the plant.

where t_f is the time interval of simulation. It holds that $Ec(\text{GKYP}) = 0.0041\,\text{N}$ while $Ec(\text{KYP}) = 0.0071\,\text{N}$. Because of that, less energy is consumed by the actuators under the controller GKYP.

Simulation for Case B

In this case, sensors and actuators are placed on different sites in the rectangular plate. A force actuator is placed at the first node of the plate, thus $\boldsymbol{b} = [1, \underbrace{0, \ldots, 0}_{n-1}]^T$. A sensor is put on the fourth node on the plate, so $\boldsymbol{c} = [\underbrace{0, \ldots, 0}_{9}, 1, \underbrace{0, \ldots, 0}_{n-10}]$. The state matrix is the same as it in Case A. The frequency response of the noncollocated plant is depicted in Figure 9.

The phase shift is beyond -90° when $\omega = 313.7\,\text{rad/s}$, which shows that the passivity of the plant is violated when $\omega > 313.7\,\text{rad/s}$. Since the GKYP controller uses the same parameters $\boldsymbol{A}_c$ and $\boldsymbol{B}_c$ as the KYP controller, the weights of the LQR algorithm are set as $\boldsymbol{Q} = 100 \times \mathbf{1}$, $\boldsymbol{Q}_c = 1 \times \mathbf{1}$ and $\boldsymbol{R} = 0.01 \times \mathbf{1}$, where $\mathbf{1}$ is an identity matrix with suitable size required by the LQR algorithm. Figure 10 depicts the time response of the four corners' displacement. The system is destabilized by the globally SPR design. It is undoubtedly due to the passivity

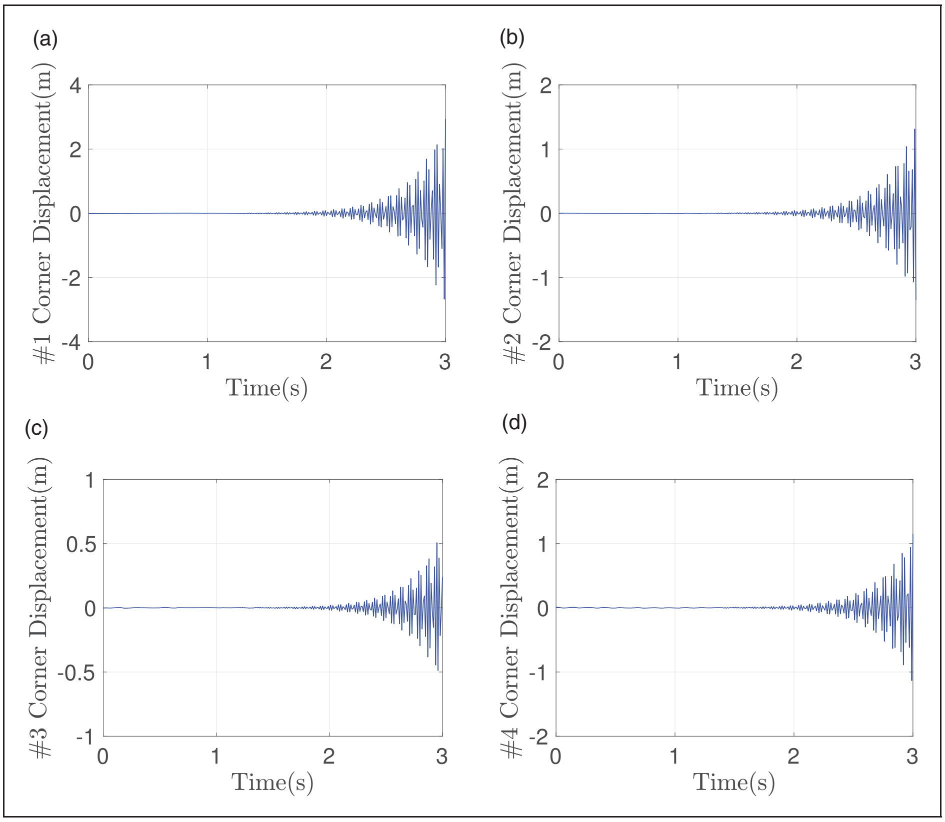

Figure 10. Displacements of four plate corners with KYP controller: (a) #1 corner; (b) #2 corner; (c) #3 corner; (d) #4 corner.

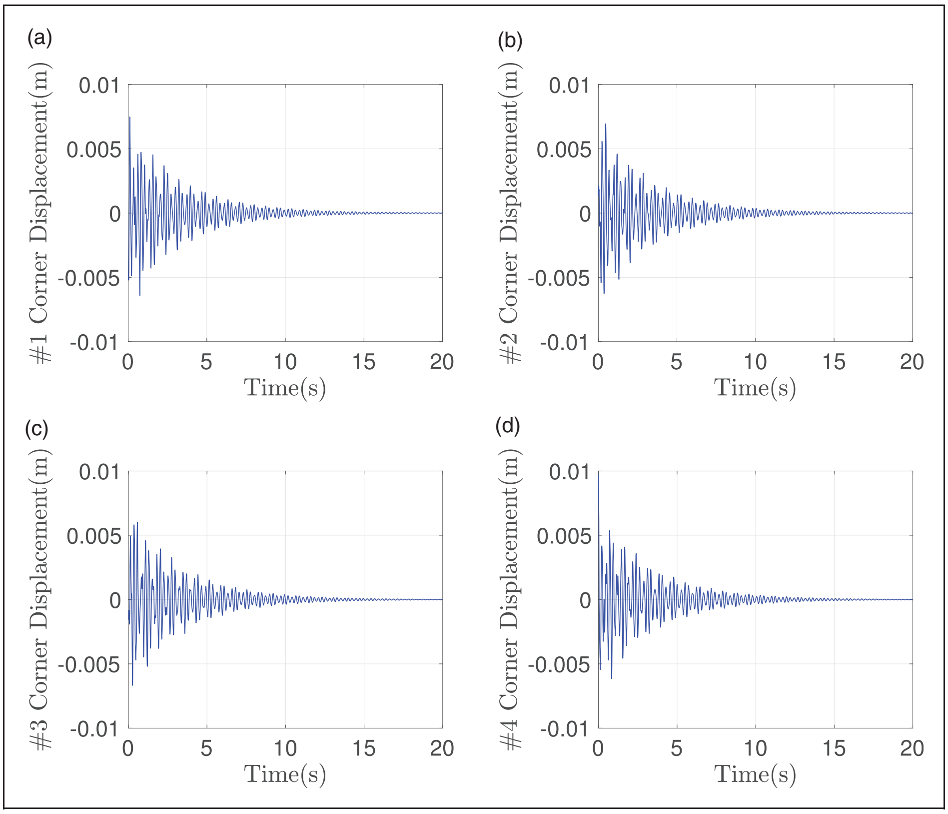

Figure 11. Displacements of four plate corners with GKYP controller: (a) #1 corner; (b) #2 corner; (c) #3 corner; (d) #4 corner.

violation. However, with the same parameters $\boldsymbol{A}_c$ and $\boldsymbol{B}_c$, the GKYP controller can stabilize the system as shown in Figures 11 and 12. The critical frequency is picked as 279.5rad/s which matches with the passive range for the plant. The gain γ_1 is obtained by evaluating the gain peak of the plant beyond ω_c from Figure 9. Since $\gamma_2 < 1/\gamma_1$, we pick the limiting gain $\gamma_2 = 7.7012$ for the controller. The controller's frequency response is shown in Figure 13. The gain of the controller is decaying when $\omega > \omega_c$.

The simulation results in both cases use the first 13 modes to build the state-space equation in (1). The GKYP controller is also based on these reduced-order modal equations. However, this controller is still effective if it is applied to a model with more modes. For Case A (collocation case), the stability of the closed-loop system will be guaranteed by the passivity theorem no matter how many modes are considered. For Case B (noncollocation case), we will demonstrate the effectiveness of the controller by applying it to a model that is built using the first one hundred modes, which is given by

$$\dot{\boldsymbol{x}} = \boldsymbol{A}_m\boldsymbol{x} + \boldsymbol{B}_m\boldsymbol{u}, \quad \boldsymbol{y} = \boldsymbol{C}_m\boldsymbol{x} \tag{42}$$

where $\boldsymbol{A}_m$, $\boldsymbol{B}_m$, and $\boldsymbol{C}_m$ are calculated using the same approach shown in equation (28) but considering one hundred modes. The controller is the same as equation (29) and synthesized using the first 13 modes

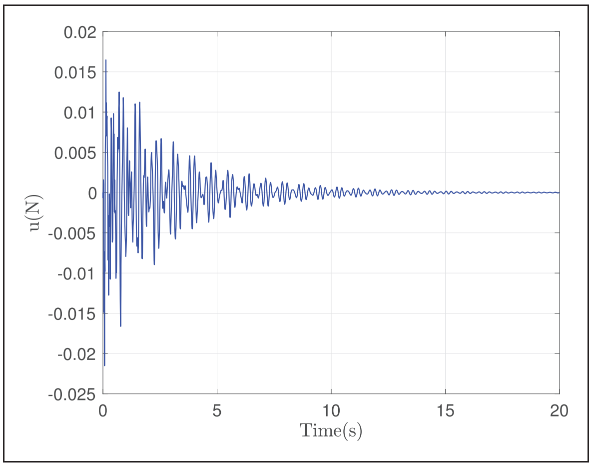

Figure 12. Control force.

as presented before. Combining the new higher order state-space equation (42) and the GKYP controller (29) gives

$$\begin{bmatrix} \dot{\boldsymbol{x}} \\ \dot{\boldsymbol{x}}_c \end{bmatrix} = \underbrace{\begin{bmatrix} \boldsymbol{A}_m & -\boldsymbol{B}_m\boldsymbol{K} \\ \boldsymbol{B}_c\boldsymbol{C}_m & \boldsymbol{A}_c \end{bmatrix}}_{\boldsymbol{A}_{com}} \begin{bmatrix} \boldsymbol{x} \\ \boldsymbol{x}_c \end{bmatrix} \tag{43}$$

The eigenvalues of $\boldsymbol{A}_{com}$ were checked and $\mathrm{Re}\{\lambda\{\boldsymbol{A}_{com}\}\} < 0$. This confirms the stability of the

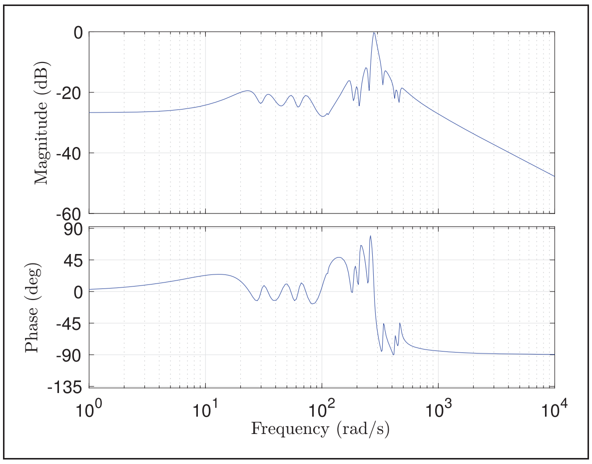

Figure 13. Frequency response for GKYP controller.

closed-loop system when the proposed control scheme is applied to a higher order modal model.

Conclusions

In this paper, a hybrid finite frequency controller has been presented for control of large flexible structures. Compared with the infinite frequency controller based on the KYP lemma, the hybrid finite frequency controller is more efficient. This controller can consume less energy to get approximately identical performance. When the standard KYP design failed to stabilize a large flexible structure when noncollocation destroyed its passivity, the hybrid finite frequency controller was still able to suppress the vibration of the plate. Here, robustness to spillover was achieved by limiting the gain (not the phase) at higher frequencies beyond the critical value. The numerical simulation demonstrated the effectiveness of the proposed controllers.

Declaration of Conflicting Interests

The author(s) declared no potential conflicts of interest with respect to the research, authorship, and/or publication of this article.

Funding

The author(s) received no financial support for the research, authorship, and/or publication of this article.

ORCID iD

Xiaoyu Lang http://orcid.org/0000-0002-4813-5276

References

1. Damaren CJ. Passivity analysis for flexible multilink space manipulators. *J Guid Control Dyn* 1995; 18: 272–279.
2. Damaren CJ. An adaptive controller for two cooperating flexible manipulators. *J Field Robot* 2003; 20: 15–21.
3. Yu S, Yu X, Shirinzadeh B, et al. Continuous finite-time control for robotic manipulators with terminal sliding mode. *Automatica* 2005; 41: 1957–1964.
4. Luo B, Huang H, Shan J, et al. Active vibration control of flexible manipulator using auto disturbance rejection and input shaping. *Proc IMechE, Part G: J Aerospace Engineering* 2014; 228: 1909–1922.
5. Balas MJ. Direct velocity feedback control of large space structures. *J Guid Control Dyn* 1979; 2: 252–253.
6. Damaren CJ and D'Eleuterio MT G. Optimal control of large space structures using distributed gyricity. *J Guid Control Dyn* 1989; 12: 723–731.
7. Hu Q. Variable structure maneuvering control with time-varying sliding surface and active vibration damping of flexible spacecraft with input saturation. *Acta Astronaut* 2009; 64: 1085–1108.
8. Hu Q, Jia Y and Xu S. Adaptive suppression of linear structural vibration using control moment gyroscopes. *J Guid Control Dyn* 2014; 37: 990–996.
9. Zhang Y and Guan X. Active damping control of flexible appendages for spacecraft. *Aerosp Sci Technol* 2018; 75: 237–244.
10. Mastory CG and Chalhoub NG. Enhanced structural controllers for non-collocated systems. *J Vib Control* 2016; 22: 678–694.
11. Shahravi M and Azimi M. A comparative study for collocated and non-collocated sensor/actuator placement in vibration control of a maneuvering flexible satellite. *Proc IMechE, Part C: J Mechanical Engineering Science* 2015; 229: 1415–1424.
12. Ferrari G and Amabili M. Active vibration control of a sandwich plate by non-collocated positive position feedback. *J Sound Vib* 2015; 342: 44–56.
13. Kulesza Z. Virtual collocation method for a flexible rotor supported by active magnetic bearings. *J Vib Control* 2015; 21: 1522–1538.
14. Oveisi A, Jeronimo MB and Nestorović T. Nonlinear observer-based recurrent wavelet neuro-controller in disturbance rejection control of flexible structures. *Eng Appl Artif Intell* 2018; 69: 50–64.
15. Forbes JR and Damaren CJ. Hybrid passivity and finite gain stability theorem: stability and control of systems possessing passivity violations. *IET Control Theory Appl* 2010; 4: 1795–1806.
16. Griggs WM, Anderson BD and Lanzon A. A "mixed" small gain and passivity theorem in the frequency domain. *Syst Control Lett* 2007; 56: 596–602.
17. Griggs WM, Anderson BD, Lanzon A, et al. Interconnections of nonlinear systems with "mixed" small gain and passivity properties and associated input–output stability results. *Syst Control Lett* 2009; 58: 289–295.
18. Forbes JR and Damaren CJ. Single-link flexible manipulator control accommodating passivity violations: theory and experiments. *IEEE Trans Control Syst Technol* 2012; 20: 652–662.
19. Forbes JR and Damaren CJ. Synthesis of optimal finite-frequency controllers able to accommodate passivity violations. *IEEE Trans Control Syst Technol* 2013; 21: 1808–1819.
20. Benhabib R, Iwens R and Jackson R. Stability of large space structure control systems using positivity concepts. *J Guid Control Dyn* 1981; 4: 487–494.
21. Iwasaki T and Hara S. Generalization of Kalman-Yakubovic-Popov lemma for restricted frequency

inequalities. In: *Proceedings of the 2003 American control conference*, vol. 5, pp.3828–3833. New York: IEEE.
22. Iwasaki T and Hara S. Generalized KYP lemma: unified frequency domain inequalities with design applications. *IEEE Trans Autom Control* 2005; 50: 41–59.
23. Marquez HJ. *Nonlinear control systems: analysis and design*. Hoboken, NJ: John Wiley & Sons, Inc., 2002.
24. Goodwin GC, Graebe SF and Salgado ME. *Control system design*. Englewood Cliffs, NJ: Prentice-Hall, 2001.